Electrochemical Removal of Remazol Black 5 (RB-5) Using SiO_2/NiO/Ni Nanocomposite Electrocatalyst Deposited on the Surface of Graphite Electrodes

Ni Made Wiratini
Departement of Chemistry, Universitas Gadjah Mada

Trisunaryanti, Wega
Departement of Chemistry, Universitas Pendidikan Ganesha

Triyono
Departement of Chemistry, Universitas Gadjah Mada

Kuncaka, Agus
Departement of Chemistry, Universitas Gadjah Mada

Electrochemical Removal of Remazol Black 5 (RB-5) Using SiO₂/NiO/Ni Nanocomposite Electrocatalyst Deposited on the Surface of Graphite Electrodes

Ni Made Wiratini[1,2], Wega Trisunaryanti[2*], Triyono[1], Agus Kuncaka[1]

[1]Departement of Chemistry, Universitas Gadjah Mada, Yogyakarta, Indonesia
[2]Departement of Chemistry, Universitas Pendidikan Ganesha, Singaraja, Indonesia

*E-mail: wegats@ugm.ac.id

Abstract: The SiO₂/NiO/Ni nanocomposite electrocatalyst was prepared by the electrodeposition method. The characterization results of SEM-EDX, TEM, FT-IR, and XRD showed that SiO₂/NiO/Ni nanocomposite electrocatalyst was deposited on the graphite surface. Furthermore, the G/SiO₂/NiO/Ni nanocomposites had higher electrocatalytic activity and surface area than that of graphite. The optimal condition for electrochemical removal of RB-5 using G/SiO₂/NiO/Ni electrode was reached at 0.05 M NaCl and pH 4 for 60 min with 100% absorbance removal efficiency. The highest COD removal efficiency of 92.85% was obtained with G/SiO₂/NiO/Ni, while the lowest of 67.57% was achieved using graphite electrodes. Based on the LC-MS analysis results, the electrochemical removal of RB-5 produced naphthalene, aromatic, and aliphatic compounds.

Keywords: SiO₂/NiO/Ni nanocomposite; electrocatalyst; deposited; graphite; electrochemical removal; RB-5 dye

1. Introduction

The textile industry is a major contributor to water pollution, with more than 100,000 types of commercial dyes manufactured annually worldwide, totaling 7,105 tonne[1]. RB-5 is a dye that is commonly used in the industry and is composed of azo-based ($-N=N-$) chromophores combined with sulfonate ($-SO_3^-$) groups. However, the reduction of the ($-N=N-$) bond in RB-5 produces amine compounds that are even more carcinogenic than the original[2]. Therefore, treatment is necessary before discharging RB-5 into the environment.

Several methods have been used to treat textile dyes including physical treatments such as membrane filtration, adsorption, ion exchange, and electrokinetic coagulation. Meanwhile, chemical methods include oxidative processes, ozonation, and phytochemical or photocatalysis[3,4,5]. The biological techniques commonly used comprise degradation with aerobic and anaerobic microbes[6]. The coagulation/flocculation and biological processes produce sludge, ozonation has a limited life, and membrane filtration is quite expensive. Therefore, an effective, efficient, and cost-effective technique for processing textile dyestuffs is needed.

Electrochemical removal is a textile dyestuff degradation technology that is efficient, cost-effective, environmentally friendly, practical, easy to operate, and does not cause sludge production. In the electrochemical process, textile dyes react with hydroxyl radicals (•OH) and degrade organic matter into CO₂ and H₂O, while hydroxyl radicals (•OH) are produced on the anode surface by direct oxidation of water[7].

However, the anode electrode material is the main factor affecting the performance of the process. Electrode modification is required for remarkable electrocatalytic activity, high oxygen evolution potential, excellent service life, and good conductivity[8].

Based on previous reports, several types of electrodes are used for textile wastewater electrochemical removals such as metal anode electrodes, dimensionally stable anode (DSA), graphite, and BDD. The most prevalent active anode is graphite, which has a low oxygen evolution potential, causes incomplete oxidation of organic pollutants, and has a high average corrosion rate[9]. To overcome this, the graphite electrode needs to be modified by the addition of an electrocatalyst to enhance the degradation of the dye. One approach is to modify the electrode with a metal oxide or deposit an electrocatalyst during the electrochemical degradation process of the dye, culminating in increased degradation results[10].

Electrocatalysts with strong catalytic activity for the anodic and cathodic reactions are nickel oxide and nickel[11]. Several nickel-based catalysts have been synthesized such as NiO/FTO/Glass, OM-NiO, RGO-Ni, NiCo₂O₄, Ni nanowire arrays, Ni alloys (Ni-Rh, Ni-Zn, Ni-Co, Ni-Zn-Co), Ni-P/RGO, and nickel coating on

stainless steel[12].

Composite catalysts can enhance electrocatalytic activity, surface area, hardness, and corrosion resistance[13,14]. Phenol degradation with Fe_3O_4/graphite composites showed an increase in yields[15]. Co_3O_4/graphite composites demonstrated excellent activity for the oxidation of 20 mg.L^{-1} diuron with 100% degradation efficiency[16]. Furthermore, the SiO_2-modified semiconductor is effective in degrading toxic chemicals because it has a large specific surface, the material is cheaper than other oxides, very stable, and can be used repeatedly[17,18]. The Co_3O_4-SiO_2/stainless steel composite electrode showed excellent catalytic activity in the oxygen evolution reaction (OER)[19]. Ni–SiO_2/CP composite electrodes exhibited specific surface, catalytic activity, and high stability on hydrogen peroxide electro-oxidation[13]. This study was conducted to examine the depositing of SiO_2/NiO/Ni nanocomposite electrocatalysts on graphite electrodes to improve the electrocatalytic properties of graphite. The deposited SiO_2/NiO/Ni nanocomposite electrocatalyst on the surface of graphite electrodes is a capable technology to increase the catalytic activity and stability of the electrode. Based on the above background, SiO_2/NiO/Ni nanocomposite electrocatalyst was deposited on graphite synthesized by the electrodeposition method. The advantages of this method are a large deposition surface area, more homogeneous particle distribution, easy implementation, automation, low cost, and fast deposition rate[20]. Moreover, the SiO_2/NiO/Ni nanocomposite electrocatalyst has the advantages of high surface area and high electrocatalytic activity. This study is based on a previous investigation[21], which examined SiO_2/NiO/Ni nanocomposite electrocatalyst deposited at graphite electrode for the electrochemical removal of RB-5. The effects of the experimental conditions explored are the electrochemical removal process duration, pH, and concentration of NaCl electrolyte solution.

2. Material and Methods

2.1 Material

The materials used for the investigation were $NiSO_4·6H_2O$ (Sigma Aldrich, > 98%), H_2O_2 (Merck, 30%), TMOS (SCIP, 99%), ethanol (Merck, 99.7%), NaCl (Merck, ≥ 99.5%), H_2SO_4 (Merck, 98%), graphite electrode (SCIP, 99.9%), RB-5 (Sigma Aldrich, ≥ 50%), KOH (Merck, 85%), KCl (Merck, 99.5%), $K_2Cr_2O_7$ (Merck, 99.9%), EDTA (AR/ACS, 99.4%), NaOH (Merck, 95%), Ag_2SO_4 (Merck, 99.5%), Hg_2SO_4 (Merck, 98%), and HCl (Merck, 37-38%).

2.2 Synthesis of SiO_2/NiO/Ni nanocomposite electrocatalyst

The synthesis of SiO_2/NiO/Ni nanocomposite electrocatalyst was modified from the results of previous studies[13]. This was achieved using Ni and SiO_2 electrodeposition methods. The total volume of the deposition solution was 50 mL, which consisted of 0.5 M $NiSO_4.6H_2O$, 0.1 M KCl, 0.4− 0.5 EDTA, CH_3CH_2OH, and 0.05 mL of TMOS homogenized with a stirrer for 15 min at 100 rpm. Furthermore, the electrodeposition process was conducted at pH 10, using a DC power supply of 1 volt for 300 min with graphite electrodes as the anode and cathode. The SiO_2/NiO/Ni nanocomposite electrocatalyst deposited on the surface of graphite electrodes namely G/SiO_2/NiO/Ni electrodes were then heated at 400ºC for 30 min. A similar process was conducted for the synthesis of NiO/Ni electrocatalyst but without the addition of CH_3CH_2OH and TMOS. The NiO/Ni electrocatalyst deposited on the surface of graphite electrodes was called G/NiO/Ni. The characterization of graphite, G/NiO/Ni, and G/SiO_2/NiO/Ni electrodes was carried out using XRD, SEM-EDX, TEM, FT-IR, GSA, and cyclic voltammetry.

2.3 Electrochemical removal of RB-5 dye

The electrochemical removal process of RB-5 dye using G/SiO_2/NiO/Ni was carried out by varying the operational parameters, duration, pH, and concentration of NaCl solution. 100 ppm RB-5 was subjected to the process at voltage 9 volt and 0.025 M NaCl as an electrolyte solution for 15, 30, 45, 60, and 90 min. The G/SiO_2/NiO/Ni composite was used as the anode, while the cathode was graphite. The removal of RB-5 with pH variations of 4, 6, and 8 was performed under optimal conditions at the electrochemical removal duration process. The process was further conducted under varying NaCl electrolyte solution concentrations of 0.00625, 0.0125, 0.025, 0.05, and 0.1 M at optimal pH conditions. The same treatment was also carried out for graphite and G/NiO/Ni anodes. The products obtained were filtered, then COD and absorbance were measured by UV-vis spectrophotometer. The filtrate was also identified by LC-MS, while optimal removal was determined by calculating the largest removal efficiency absorbance and COD for each variation. COD removal efficiency on RB-5 electrochemical removal was calculated using Equation 1, where C_i and C_f are COD values of RB-5 before and after electrochemical removal respectively.

$$\text{COD removal efficiency (\%)} = \frac{C_i - C_f}{C_i} \times 100 \qquad (1)$$

3. Results and Discussion

3.1 Characterization of G/NiO/Ni and G/SiO_2/NiO/Ni using X-ray diffraction, FT-IR, SEM-EDX, TEM, GSA, and cyclic voltammetric

The characterization of G/NiO/Ni and G/SiO_2/NiO/Ni using XRD is shown in Fig. 1. The XRD pattern showed that NiO/Ni and SiO_2/NiO/Ni nanocomposite electrocatalysts were deposited on the graphite electrode. Fig. 1 shows that the peaks at 2θ = 26.5º (002) and 2θ = 54.6º (004) are characteristics of graphite. These results

are in accordance with a previous study[22]. Furthermore, the XRD diffractograms of G/NiO/Ni (Fig. 1(b)) and G/SiO$_2$/NiO/Ni (Fig. 1(c)) showed the emergence of four new diffraction peaks at $2\theta = 43.5°$; $63.1°$; and $75.4°$ which is characteristic of NiO as well as $2\theta = 51.9°$ representing Ni. In the G/SiO$_2$/NiO/Ni diffractogram shown in Fig. 1(c), there was a new diffraction peak at $2\theta = 21.98°$ which represents SiO$_2$. The diffraction peak at $2\theta = 43.5°$; $63.1°$; $75.4°$ indicates NiO, while $2\theta = 51.9°$ and $2\theta = 22°$ are characteristic of Ni and SiO$_2$ respectively (JCPDS No. 70-0989)[23].
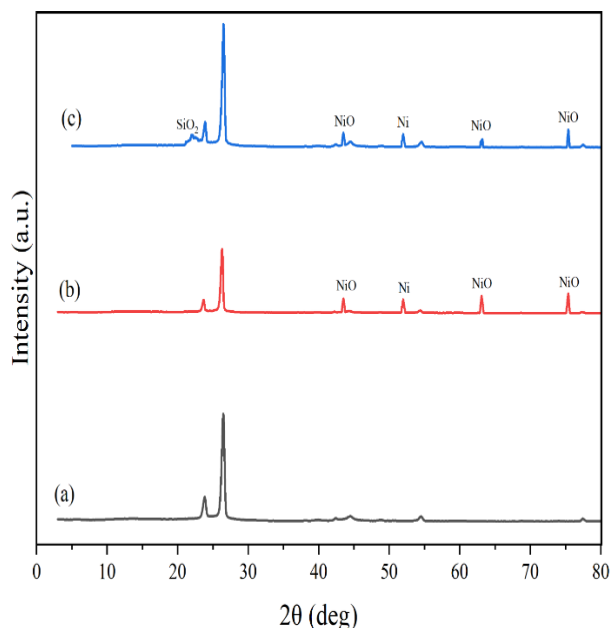

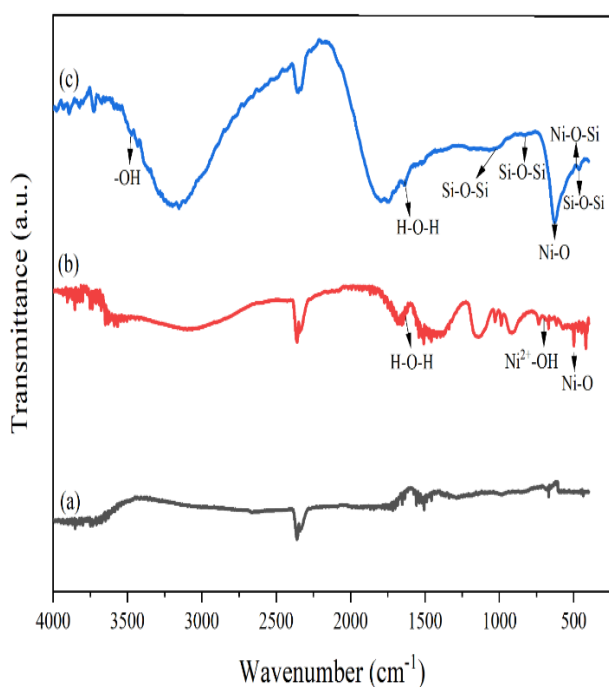**Fig. 1:** XRD pattern of graphite (a), G/NiO/Ni (b), and G/SiO$_2$/NiO/Ni (c).

Fig. 2: FTIR spectrum of graphite (a), G/NiO/Ni (b), and G/SiO$_2$/NiO/Ni (c).

Spectroscopic characterization of the graphite electrode, G/NiO/Ni, and G/SiO$_2$/NiO/Ni in the range of 500 - 4,000 cm^{-1} are presented in Fig. 2. The spectra FT-IR of G/SiO$_2$/NiO/Ni (Fig. 2(c)) exhibited a peak at 3,474 cm^{-1} which was related to the silanol SiOH and showed stretching vibration (O−H) present on the silica surface. At peak 1,635 cm^{-1} the spectra showed stretch (H−O−H) of the water angular vibrations deformation, while at 1,097 cm^{-1} and 807 cm^{-1} there were asymmetrical and symmetrical stretch vibrations (Si−O−Si), at 610 cm^{-1} indicating Ni−O, as well as 484 cm^{-1} and 474 cm^{-1} representing the formation of Ni-O-Si structure and vibrational bending (Si−O−Si) respectively. The spectra FTIR of G/NiO/Ni (Fig. 2(b)) showed the emergence of a peak at 1,635 cm^{-1} which indicated stretch vibrations of H−O−H. At a peak of 700 cm^{-1} it indicated stretching (Ni^{2+}−OH), and 500 cm^{-1} represented (Ni−O). A previous study stated that at a peak of 484 cm^{-1}, Ni^{2+} entered the SiO$_2$ framework, and a Ni-O-Si structure was formed. Additionally, it exhibited stretch (H−O−H) at 1,635 cm^{-1}, asymmetrical and symmetrical stretch vibration (Si-O-Si) at 1,097; 1,105; 962; and 807 cm^{-1}, Ni−O was formed between 610 and 480 cm^{-1}, stretching vibration (O-H) appeared between 3,450 and 3,500 cm^{-1}, bending vibration of cyclic Si−O−Si at 474 cm^{-1}, and stretching (Ni^{2+}−OH) appeared at 700 cm^{-1} [17].
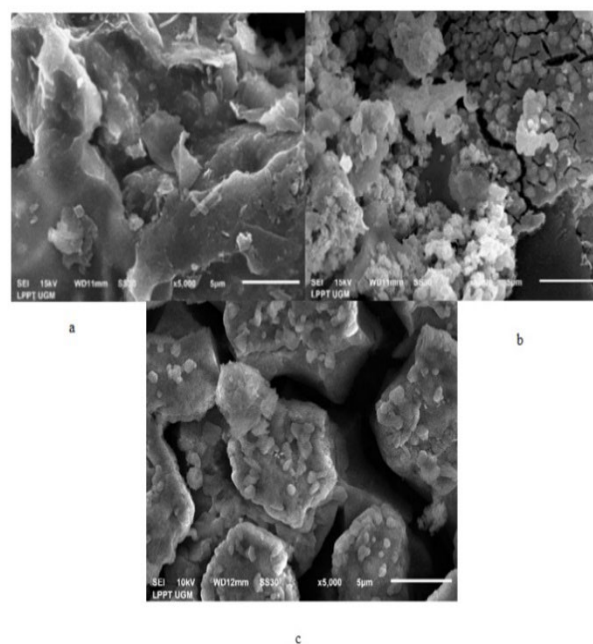

Fig. 3: SEM images of graphite (a), G/NiO/Ni (b), and G/SiO$_2$/NiO/Ni (c).

Characterization results of the graphite, G/NiO/Ni, and G/SiO$_2$/NiO/Ni electrode using SEM are shown in Fig. 3. The SEM result revealed that the surface of graphite had been coated by NiO, Ni, and SiO$_2$. Fig. 3(a) shows a plain surface of the graphite electrode, while Fig. 3(b) and 3(c) indicated that Ni, O, and Si particles are scattered on the surface of the graphite in the form of granular, spherical, solid, and cracks.
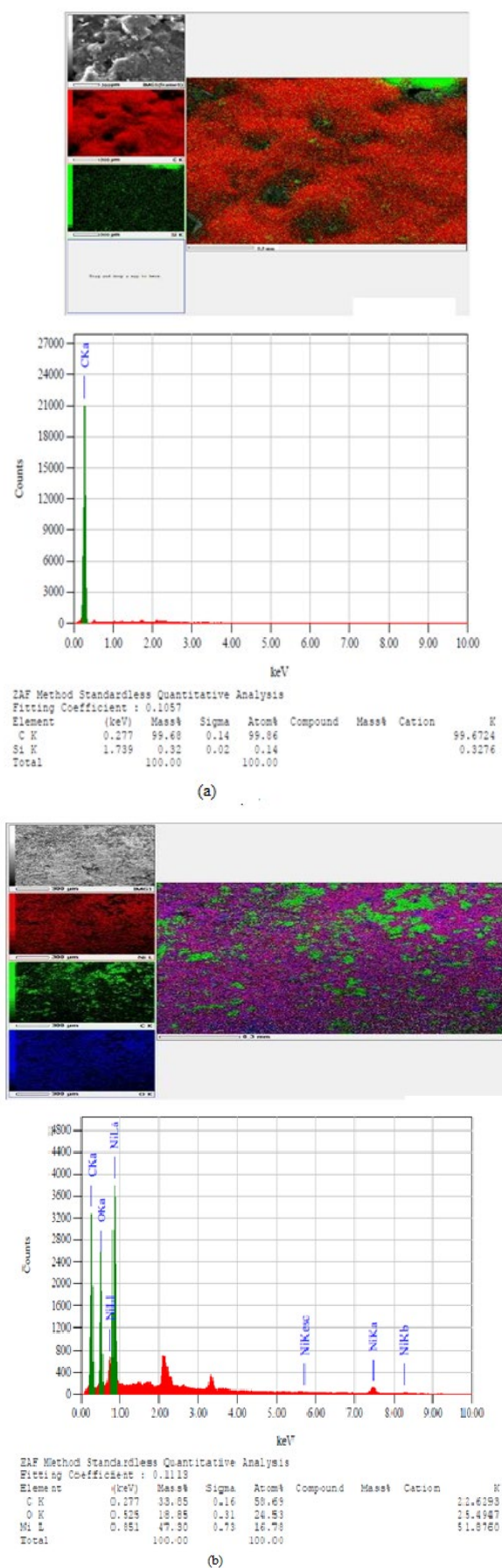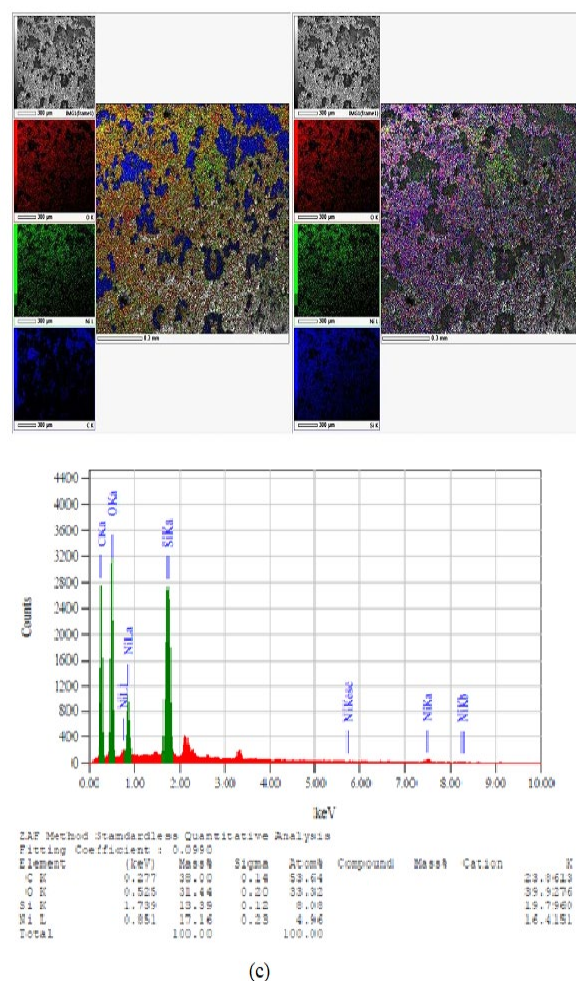
Fig. 4b: EDX spectrum of $G/SiO_2/NiO/Ni$ (c).

A granular form suggests a high surface area, while the cracks are associated with contraction during drying due to tensile stress[20]. After electrodeposition with $SiO_2/NiO/Ni$ electrocatalyst (Fig. 3(c)), the cracks widened with NiO/Ni infiltrating the cavity. Similar results were also reported in SiO_2 as shown in the form of solid spherical particles[13], round and cracked with NiO infiltrating the cavity[24].

Confirmation of the presence of Ni, Si, and O elements as materials deposited on the graphite electrode was determined by EDX analysis. The analysis results showed that the deposited material consists of the elements Ni, Si, and O, while Fig. 4 and Table 1 present complete information related to the results of the EDX analysis. The percentages of Ni and O in the G/NiO/Ni were higher than in the $G/SiO_2/NiO/Ni$. This is consistent with the SEM results of the $G/SiO_2/NiO/Ni$. Fig. 3(c) shows that NiO/Ni infiltrated into the cavity to enlarge the crack. The enlarged crack structure caused a decrease in the amount of NiO/Ni on the surface of the graphite electrode.

Fig. 5 shows the characterization of G/NiO/Ni and $G/SiO_2/NiO/Ni$ using TEM at 20 and 50 nm magnification. The TEM result revealed that the NiO/Ni and $SiO_2/NiO/Ni$ electrocatalysts are nanostructured, while Fig. 5(a) shows NiO/Ni electrocatalyst deposited on the

Fig. 4a: EDX spectrum of graphite (a) and G/NiO/Ni (b)

surface of the graphite electrode, composed of a sheet-like film interspersed with black beads. After the electrodeposition of the SiO₂/NiO/Ni electrocatalyst (Fig. 5(b)), the number of black beads decreased, possibly indicating that they were NiO/Ni. Fig. 5(b) shows a SiO₂/NiO/Ni electrocatalyst on the graphite surface, composed of a sheet-like film which is more spread than that of Fig. 5 (a). These results are in accordance with a previous study[13].
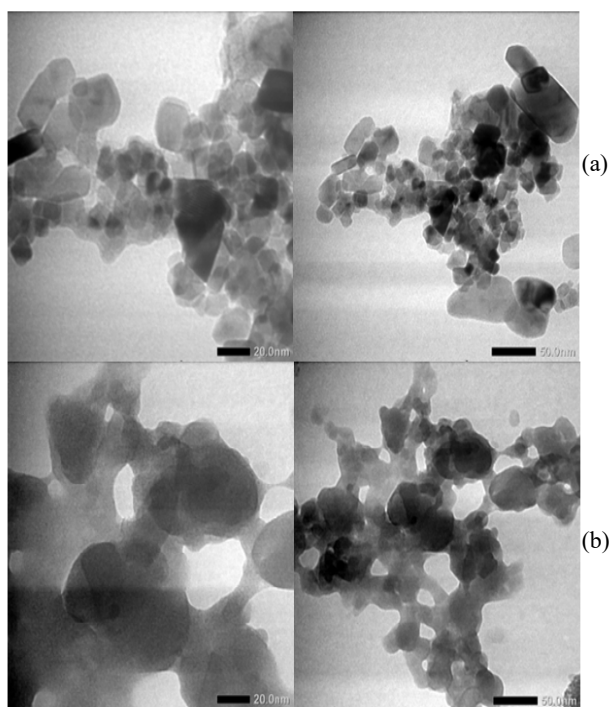

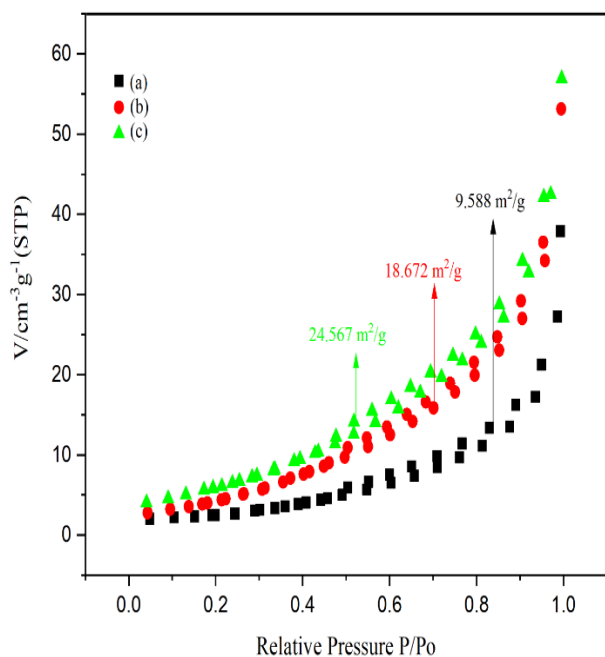**Fig. 5:** TEM images of the G/NiO/Ni (a) dan G/SiO₂/NiO/Ni (b).

Fig. 6: The nitrogen adsorption-desorption isotherms of graphite (a), G/NiO/Ni (b), and G/SiO₂/NiO/Ni (c).
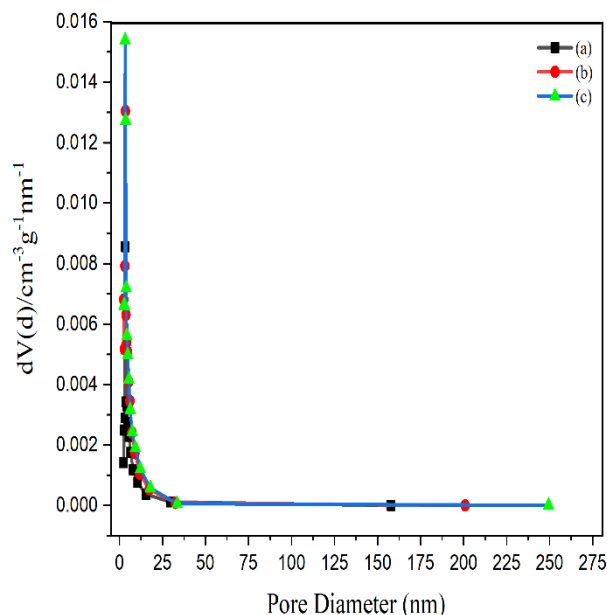

Fig. 7: The pore diameter distributions of graphite (a), G/NiO/Ni (b), and G/SiO₂/NiO/Ni (c) assessed by BJH.

Fig. 6 shows a type (IV) adsorption/desorption isotherm curve according to IUPAC with a hysteresis loop at relatively high pressure indicating capillary condensation in mesoporous materials[6]. Table 2 and Fig. 6 reveal that G/SiO₂/NiO/Ni electrodes have the greatest potential for RB-5 electrochemical removal reactions. Pore size distribution of graphite, G/NiO/Ni, and G/SiO₂/NiO/Ni electrodes was obtained by applying the Barrett–Joyner–Halenda (BJH) model, as shown in Fig. 7 and Table 2. The graphite, G/NiO/Ni, and G/SiO₂/NiO/Ni electrodes are mesoporous materials with a relatively uniform pore size distribution of 2-15 nm. Table 2 reveals that the pore volume of G/SiO₂/NiO/Ni electrodes was the highest compared to graphite and G/NiO/Ni. This result is very beneficial for catalyzing the electrochemical removal of RB-5. The higher the specific surface area and pore volume, the more conducive the electrodes, and the greater their potential for catalyzing the electro-oxidation of hydrogen peroxide[13].

Table 1. Comparison percentage of mass and atom from SEM-EDX analysis

No	Anode material	%	C	O	Si	Ni
1	Graphite	Mass	99.68	0.00	0.32	0.00
		Atom	99.86	0.00	0.14	0.00
2	G/NiO/Ni	Mass	33.85	18.85	0.00	47.30
		Atom	58.69	24. 53	0.00	16.78
3	G/SiO₂/NiO/Ni	Mass	38.00	31.44	13.39	17.16
		Atom	53.64	33.32	8.08	4.96

Based on Fig. 8, the current limiting and response of G/NiO/Ni and G/SiO₂/NiO/Ni are higher than those of graphite. This suggests that the surface area of the

G/NiO/Ni and G/SiO$_2$/NiO/Ni was more actively charged, making the Cl$^-$ oxidation reaction more likely to occur. Therefore, the electrocatalytic activity of both materials was higher than that of graphite. The high limiting current of the voltammogram indicates that the electrode surface had a more active charge thereby increasing the electrocatalytic activity[25]. According to a previous study, the Cl$^-$ oxidation reaction by the electrode easily occurs when the voltammogram presents a high current response[26].

Table 2. Porous structure characterization of the different anode

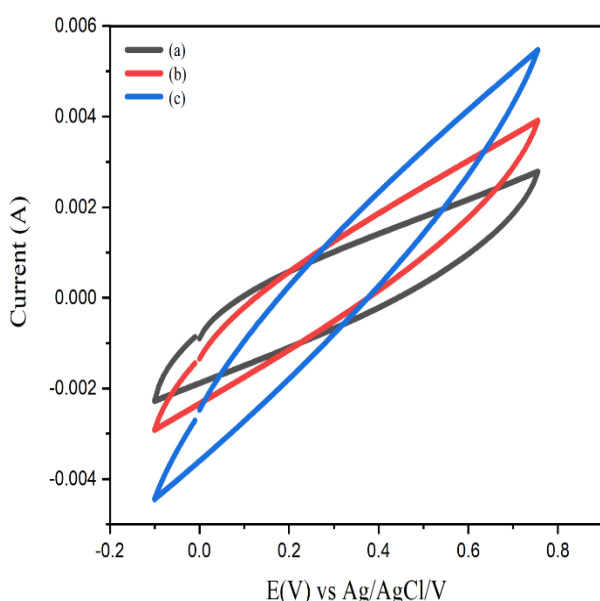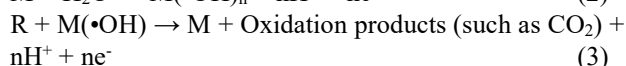| No	Anode material	BET Surface Area (m^2/g)	Total Pore Volume (cm^3/g)	BJH Desorption Average Pore Diameter (nm)
1	Graphite	9.588	0.052	12.327
2	G/NiO/Ni	18.672	0.079	9.525
3	G/SiO$_2$/NiO /Ni	24.567	0.083	9.035

Fig. 8: Voltamogram of graphite (a), G/NiO/Ni (b), and G/SiO$_2$/NiO/Ni (c) at 0.1 M NaCl and scan rate 10 mV.s^{-1}.

3.2 The effect of reaction duration, pH, and electrolyte concentration (NaCl) on absorbance reduction efficiency of RB-5

The spectrum of RB-5 before and after electrochemical removal is shown in Fig. 9((a), (b), (c)). The maximum wavelength in the visible region appeared at 595 nm, which is characteristic of the azo chromophore group (−N=N−). Meanwhile, in the UV region, the peak appeared at wavelengths 229, 254, 310, and 391 nm which represents unsaturated groups, such as the benzene, naphthalene, and heterocyclic ring[27]. During the electrochemical removal process with graphite, the peak decreased at 595 nm, while with G/NiO/Ni and

G/SiO$_2$/NiO/Ni, the absorption peak at 595 nm disappeared. This was because the chromophore groups turned into intermediates, before the formation of aliphatic carboxylic acids and carbon dioxide. This event accelerated the decrease in absorbance and removal of the peak at 595 nm[28]. The decrease in the visible region was greater than that of the UV region because the aromatic structure is more stable than the azo chromophore group. G/NiO/Ni and G/SiO$_2$/NiO/Ni electrodes increased the electrode surface area (Fig. 6), total pore volume (Table 2), and current response (Fig. 8), causing an improvement in the performance of graphite electrode in the RB-5 electrochemical removal process. Previous studies reported that the degradation of rhodamine B increased with the addition of iron silica mesoporous catalyst[29].

The electrochemical removal of RB-5 dyes using graphite, G/NiO/Ni, and G/SiO$_2$/NiO/Ni in NaCl solution occurred in two ways, namely directly and indirectly. It is directly achieved by the adsorbed hydroxyl radicals resulting from the water oxidation reaction[8], according to Equations 2 and 3 as follows:

$$M + H_2O \rightarrow M(\bullet OH)_n + nH^+ + ne^- \qquad (2)$$
$$R + M(\bullet OH) \rightarrow M + \text{Oxidation products (such as } CO_2) + nH^+ + ne^- \qquad (3)$$

Meanwhile, the indirect removal involved the degradation of NaCl solution by Cl$_2$, HClO, or OCl$^-$ ions in accordance with the pH, starting from Cl$^-$ oxidation (Equation 4), followed by reactions (5), (6), and (7)[30].

$$2Cl^- \rightarrow Cl_2 + 2 e^- \qquad (4)$$
$$Cl_2 + H_2O \rightarrow HOCl + H^+ + Cl^- \qquad (5)$$
$$HOCl \rightleftharpoons H^+ + OCl^- \qquad (6)$$
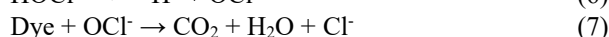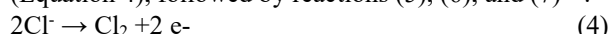$$\text{Dye} + OCl^- \rightarrow CO_2 + H_2O + Cl^- \qquad (7)$$

Fig. 9(d) shows that at 15 min, the absorbance removal efficiency values of graphite, G/NiO/Ni, and G/SiO$_2$/NiO/Ni were 48.13, 99.10, and 99.74%, while at 60 min, the values were 99.74, 99.87, and 99.94%, respectively. The percentage of RB-5 absorbance removal efficiency increased with higher duration because the longer the electrochemical removal, the greater the number of main oxidizing agents hypochlorite ions (OCl$^-$) and hydroxyl radicals (•OH) which degrade dye[31]. A previous study reported that the efficiency of decolorization of methylene blue using graphite anode coated with lead dioxide (G/β-PbO$_2$) increased with a rise in reaction time of 97.67% for 50 min and 79.67% for 10 min of the electro-oxidation process[9]. Platinum (Pt) electrodes can decolorize 88.68% of reactive blue 21 dye in water for 5 min and increase to 99.94% after 20 min of the electro-oxidation process[30].

The electrochemical removal of RB-5 at various pH was carried out for 60 min, which was found to be the most optimal duration. Fig. 10(a) shows that the absorbance removal efficiency at pH 4 for graphite, G/NiO/Ni, and G/SiO$_2$/NiO/Ni was 99.74, 99.94, and 100%, respectively. The electrochemical removal in the NaCl solution was degraded by active chlorine depending on the pH. When the pH was 3; 3-8; and more than 8, each was dominated by active chlorine Cl$_2$, HClO, and ClO$^-$

respectively. The oxidation rate of organics with active chlorine was lower in alkaline than in acidic media, due to the lower standard potential of ClO$^-$ (E^o = 0. 89 V) compared to Cl$_2$ (E^o = 1.36 V) and HClO (E^o = 1.49 V)[30]. In addition, the decline in pH decreased the oxygen evolution rate on the anode surface thereby increasing the rate of diffusion of organic pollutants to the anode. This caused an increase in the rate of organic matter oxidation on the anode surface[32].
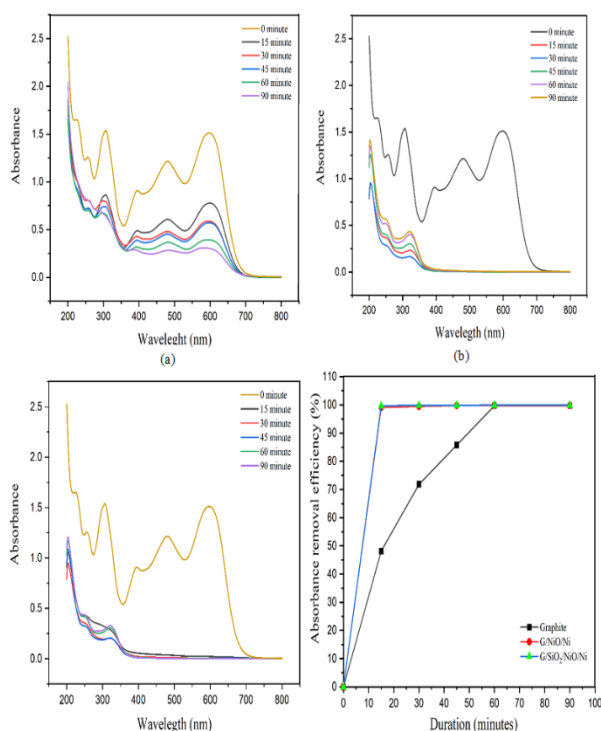
reported that the rate of electro-oxidative acid blue 80 decreased with a decline in electrolyte conductivity. Besides, electrolyte conductivity decreased when the amount of sodium chloride in wastewater was reduced. Increasing the concentration of Cl$^-$ increased the production of chlorine and decreased the selectivity for oxygen evolution thereby enhancing the electrochemical removal of RB-5 [35].

Fig. 10: The relation between pH (a), NaCl concentration (b), and the percentage of the absorbance removal efficiency 100 ppm of RB-5 dye.

Fig. 9: The absorbance spectra of the graphite (a), G/NiO/Ni (b), and G/SiO$_2$/NiO/Ni (c), the relation between electrochemical removal duration and percentage absorbance removal efficiency 100 ppm of RB-5 dye (d).

Previous studies reported that the optimal pH for the electrochemical oxidative of X-6G dye by boron-doped diamond (BDD) was 3 with 99.80% decolorization efficiency achieved after 60 min at a current density of 100 mA.cm^{-2} and 0.005 M Na$_2$SO$_4$[33]. Degradation of 100 mg.L^{-1} acid orange 7 (AO7) occurred under optimal conditions of pH 5, a current density of 20 mAcm^{-2}, and 0.1 M Na$_2$SO$_4$ for 60 min shown with a decolorization efficiency of 87.15%[34]. Furthermore, the methylene blue removal efficiency increased with decreasing pH. The removal efficiency of 60 mg.L^{-1} methylene blue was 97.67% at pH 5.75, 10 mA.cm^{-2}, and 78.8 mg.L^{-1} Na$_2$SO$_4$[9].

The electrochemical removal of RB-5 in NaCl variation was carried out at pH 4. Fig. 10(b) shows that the absorbance removal efficiency increased with rising concentrations of the NaCl solution. The improvement of NaCl concentration also increased the number of Cl$^-$ ions, causing an upsurge in the indirect electro-oxidation reaction by active chlorine (Equation 5). Previous studies
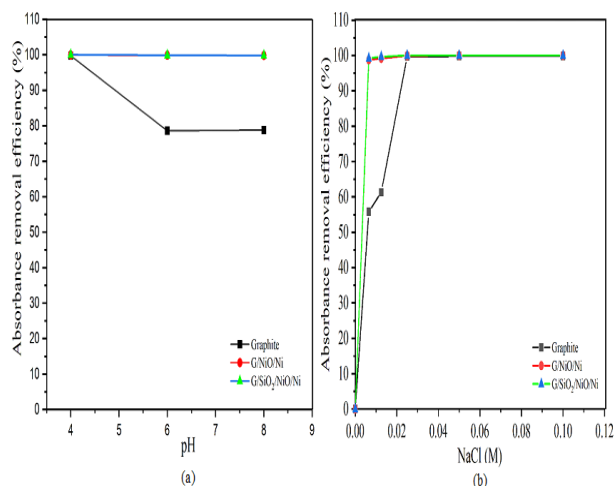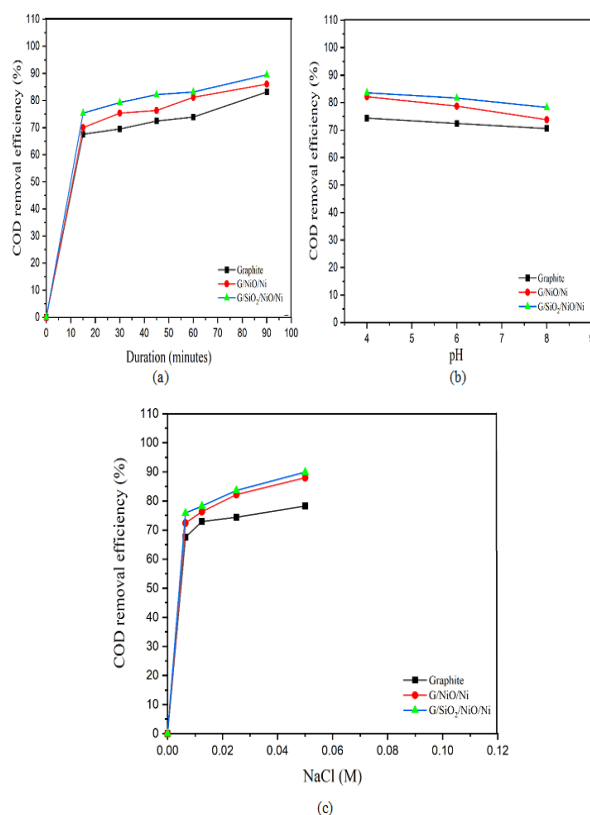

Fig. 11: The relation between duration (a), pH (b), NaCl concentration (c), and the percentage of the COD removal efficiency 100 ppm of RB-5 dye.

Fig. 10(b) shows that the absorbance removal

efficiency of graphite electrode as well as G/NiO/Ni and G/SiO$_2$/NiO/Ni are 55.81, 98.77, and 99.23% respectively at 0.00625 M NaCl concentration. The concentration of 0.05 M NaCl was found to be the most optimal with an absorbance removal efficiency of 99.81% for graphite as well as 100% for G/NiO/Ni, and G/SiO$_2$/NiO/Ni. Previous studies reported that the decolorization efficiency of Ti/Ru$_2$-IrO$_2$ and SnO$_2$ electrodes at concentrations of 0.01 M NaCl was 24 and 14%, respectively. These values increased at concentrations of 0.1 M NaCl to 87 and 44%, respectively[36]. The absorbance reduction efficiency of G/SiO$_2$/NiO/Ni reached 100% because the deposition of SiO$_2$/NiO/Ni electrocatalyst on graphite increased the catalytic activity by accelerating the half-cell reaction on the electrode surface. Similar results were also reported for the electrochemical degradation of 50 mg.L^{-1} hexazinone by PbO$_2$ anode and Bi-doped PbO$_2$ anode where the removal ratio reached 78 and 97.90%, respectively. The degradation of hexazinone by pure PbO$_2$ was significantly lower than that of Bi-doped PbO$_2$ electrode[37].

3.3 The effect of duration variation, pH, and electrolyte concentration (NaCl) on the COD reduction efficiency of RB-5

The increase in COD reduction efficiency percentage with higher electrochemical removal duration, decreasing pH, and increasing NaCl concentration is shown in Fig. 11. The decrease in COD indicates that the degradation did not only take place in the color-forming groups. According to the basic principle of COD analysis, the decrease in COD value indicates a change in the chemical compound due to the quantity of oxygen required for oxidation. A low value implies that a compound has a small quantity or a short carbon chain[34].

Table 3. Electrochemical removal of RB-5 at different electrodes reported in the literature

RB-5 (ppm)	E	A	C	Result	Ref.
70	E.time 180 min, V= 5volt, Na$_2$SO$_4$= 0.1 M, pH = n.d	Graphite	Graphite	A.Ef: 100% cylindrical cell and 84% cubic cell COD red: n.d	28)
	E.time 180 min, V= 5 volt, [NaCl]= 10 g.L^{-1}, pH = n.d	Graphite	Graphite	A.Ef: 100% cubic and cylindrical cell COD red: n.d	
50	E.time 180 min,	BDD/Ti	Pt	A.Ef: 100%	38)
	j= 74 mA.cm^{-2} [K$_2$SO$_4$]= 0.1 M, pH = 2.5			COD red: n.d	
100	E.time 60 min, j =5.5 mA.m^{-2}, [NaCl]= 4 g.L^1, pH = 2	Nb/ BDD	SS	A.Ef: n.d COD red: 90.87%	35)
		Si/BDD	SS	A.Ef: n.d COD red: 88.65%	
300	E.time: 15 min, j = 1.5 A, [NaCl] = 0.008 M, pH= n.d	Ti/RuO/ IrO$_2$/ TiO$_2$	SS	A.Ef: n.d COD red: 33%	2)
1000	E.time 120 min, j = 50 mA.cm^{-2} [NaCl]= 0.07 M, pH = 3	Ti/C$_o$O$_x$-RuO$_2$– SnO$_2$– Sb$_2$O$_5$	SS	A.Ef: 97% COD red.: n.d	31)
100	E.time 300 min, j= 15 mA.cm^{-2}, [Na$_2$SO$_4$] = 0.1 M, pH = n.d	BDD	Pt	A.Ef: n.d COD red: 35%	27)
		ceramic Sb-doped SnO$_2$	Pt	A.Ef: n.d COD red: 0%	
100	E.time 60 min, V = 9 volt, [NaCl] = 0.05 M, pH = 4	Graphite	Graphite	A.Ef: 99.81% COD red: 78.27%	this work
		G/NiO/ Ni	Graphite	A.Ef: 100% COD red: 87.99%	
		G/SiO$_2$/ NiO/Ni	Graphite	A.Ef: 100% COD red: 89.94%	

*E : Experimental conditions, *A: Anode, *C: Cathode. *A.Ef: Absorbance removal efficiency, *COD red: COD removal efficiency, *and no data, *E.time: Electrochemical removal time

Fig. 11(a) shows that the COD removal efficiency at 15 min of the RB-5 electrochemical removal process was 67.57, 70.00, and 75.35% for graphite, G/NiO/Ni, and G/SiO$_2$/NiO/Ni. Meanwhile, at 90 min, it was 83.13, 86.05, and 89.45% respectively. The prolonged electrochemical removal duration caused an increase in the number of active chlorine species (Cl$_2$/HClO/ClO$^-$), thereby increasing the COD removal efficiency. Previous studies reported that active chlorine species can increase

the oxidation of organic compounds through an indirect electrochemical oxidation mechanism, resulting in a high COD reduction in dye waste[31]. Electro-oxidation of 2-4D herbicide showed the lowest removed efficiency obtained at the minimum electrolysis time[39].

Fig. 11(b) shows that the COD removal efficiency at pH 4 was 74.38, 82.16, and 83.62% for graphite, G/NiO/Ni, and G/SiO$_2$/NiO/Ni, respectively. At this pH (acidic), the electron donors of the dye will be disturbed by H$^+$. A higher concentration of H$^+$ induced a lone pair of electrons in the dye structure, thereby reducing its strength and increasing the oxidation reaction by Cl$_2$/HClO/ClO$^-$. The reaction equilibrium between oxidizing agents (Cl$_2$/HClO/ClO$^-$) was also affected by pH. At pH 4, the abundance of HClO was higher than ClO$^-$ which is a stronger oxidizing agent than ClO$^-$. According to previous studies, the oxidation of textile wastewater achieved using cylinder Ti/β-PbO$_2$ electrode at 4000 mgL^{-1} NaCl; and 5.6 V had a higher COD removal rate at pH 6 than 9 with removal efficiency of 70 and 55%, respectively[25]. In other words, COD reduction at neutral or alkaline pH was lower than that at acidic. The maximum COD reduction of acid orange 7 dye using a PbO$_2$ electrode was 49.88% at pH 5[34]. Moreover, mineralization of acid yellow 25 dye using anode electrode Ti/Ru$_{0.3}$Ti$_{0.7}$O$_2$, for 60 min and 50 mM NaCl, obtained COD removal values of 74, 46, and 58%, respectively at pH 3, 7, and 10[10].

Fig. 11(c) shows that the highest COD removal efficiency achieved with 0.1 M NaCl was 83.13, 88.96, and 92.85% for graphite, G/NiO/Ni, and G/SiO$_2$/NiO/Ni, respectively. Meanwhile, the lowest values obtained with 0.0065 M NaCl were 67.57, 72.44, and 75.84%. Previous studies reported that COD removal improved from 64.77 to 93.60%, due to an increase in NaCl concentration in the electrolysis of 1 gL^{-1} reactive red dye with DSA (RuO$_2$-IrO$_2$/Ti) for 3 hours[40]. It also improved with higher Na$_2$SO$_4$ concentration and the value was 45.43% when 0.1 M was used in the electrochemical oxidation of acid orange 7 dye with a PbO$_2$ electrode[34].

The COD removal efficiency of graphite was lower than G/NiO/Ni and G/SiO$_2$/NiO/Ni and the results are in line with previous studies. β-PbO$_2$ electrocatalyst deposited on graphite was found to increase methylene blue removal efficiency. Furthermore, electro-oxidation of 60 mgL^{-1} methylene blue at pH 5.75 and Na$_2$SO$_4$ 78.8 mgL^{-1}, for 10 min exhibited removal efficiencies of 25 and 87% for graphite and graphite/β-PbO$_2$ anodes. Using the same experimental parameters, the value of removal efficiencies for 60 min are 68.30 and 96.40%, respectively[9].

Table 3 summarizes the results of previous studies on the electrochemical oxidation of RB-5 using different anode materials. The differences in value decolorization and COD are attributed to variations in the electrogenerated oxidants, electrode materials, applied currents, and electrolyte solutions[29]. The electrochemical removal of RB-5 with G/SiO$_2$/NiO/Ni showed that the reduction efficiency of absorbance and COD was not significantly

different compared to Nb/BDD and Si/BDD electrodes. Therefore, graphite/NiO/Ni and graphite/SiO$_2$/NiO/Ni electrode are good for electrochemical removal of RB-5. As shown in Table 3, the removal efficiency of absorbance and COD for the graphite electrode was lower than that of G/SiO$_2$/NiO/Ni and G/NiO/Ni. The deposition of NiO/Ni and SiO$_2$/NiO/Ni electrocatalysts on the surface graphite electrode (Fig.1-8) can improve the potentiality of the electrode to oxidize Cl$^-$ (Equation 4) and accelerate the reaction of Equations 5 and 6, thereby increasing the efficiency of absorbance and COD removal (Equation 7).
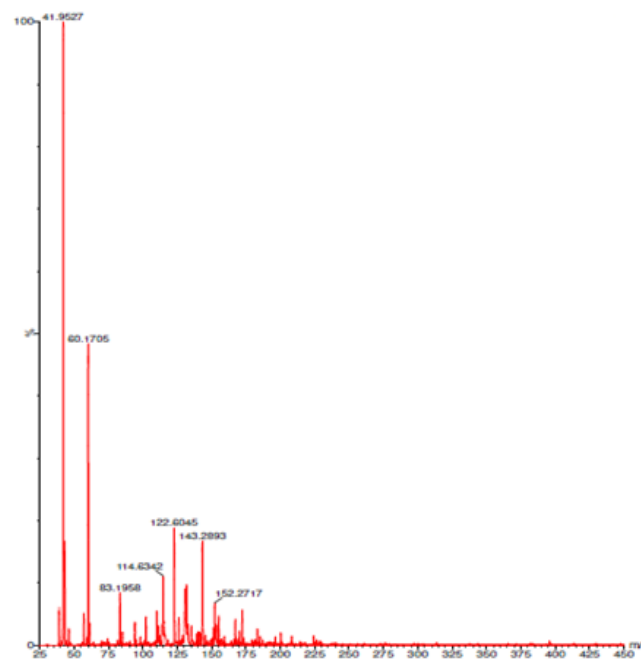

Fig. 12: Mass spectrum of RB-5 dye after electrochemical removal for 60-min using G/SiO$_2$/NiO/Ni.

Table 4. Intermediate compounds were identified by LC-MS during 60 min the RB-5 electrochemical removal using G/SiO$_2$/NiO/Ni

No	m/z (experimental)	m/z (matched with the literature)	Chemical name
1	143.16	144	Naphthalen-1-ol
2	152.27	150	2-Carboxybenzaldehyde
3	122.60	122	Benzoic acid
4	60.17	60	Acetic-acid
5	41.95	42	Keto-ethylene

3.4 LC-MS analysis

LC-MS analysis was performed to identify intermediates formed in the liquid phase during the electrochemical removal process of RB-5. The intermediates produced after 60 min are presented in Fig.

12, Fig.13, and Table 4. All these compounds are possible degradation products of partial oxidation. The LC-MS results are in line with the UV-Vis findings in Fig. 9(c). The azo chromophore groups were not detected, while the unsaturated groups remained present.
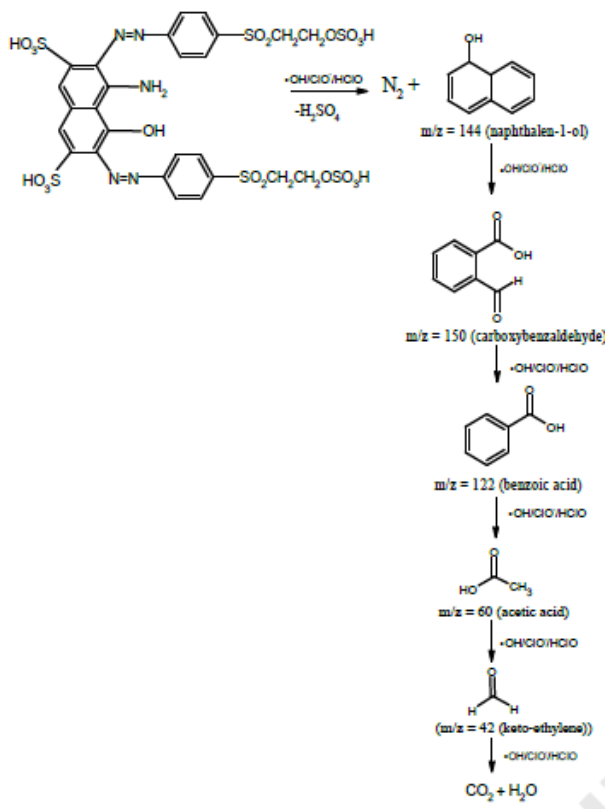

Fig. 13: The mechanism proposed for the electrochemical removal of RB-5 for 60 min using G/SiO₂/NiO/Ni

Based on Fig. 12 and 13, as well as Table 4, RB-5 can be rapidly degraded on the surface of G/SiO₂/NiO/Ni. The LC-MS spectrum showed very strong fragmentation results, with the absence of quasi-molecular ions of RB-5, which is typical for sulfonic acid esters with -O-SO₃ group[41]. The first step of degradation was the reductive rupture of the azo bond and deletion of NaSO₃ and NH₂ groups, followed by the addition of H⁺ and •OH, leading to the formation of intermediates 1. At this stage, one of the aromatics rings of intermediates 1 was ruptured, producing intermediates 2. Decarboxylation of intermediates 2 was also converted into 3. All the aromatic rings of RB-5 were ruptured, then it was oxidized and mineralized into small molecular products 4 and 5 which continue to degrade CO₂ and H₂O. Previous studies reported the results of RB-5 electrochemical oxidation with titanium-based DSA coated by mixed oxides of RuO₂/IrO₂/TiO₂. The LCMS analysis results for 160 min of electrochemical oxidation revealed the presence of azo compounds with molecular weights around 400-600 that were colorless, did not absorb at visible, quinone, and aliphatic wavelengths[7]. In contrast, the use of dimensionally stable anode Ti/CoOₓ-SnO₂–Sb₂O₅ showed

that the results after 60 min of electrolysis were m/z 223.1, 281.1, 39, 387, and 421[31].

4. Conclusion

The SiO₂/NiO/Ni nanocomposite electrocatalyst was successfully deposited on a graphite surface, as confirmed by XRD results showing characteristic peaks at 2θ = 43.5°; 63.1°; 75.4°, 2θ = 51.9°, and 2θ = 21.98° for NiO, Ni, and SiO₂. FTIR spectra at 484 cm⁻¹ indicated that the Ni-O-Si structure had formed, while SEM-EDX analysis revealed that Ni, Si, and O were deposited on the surface of the graphite electrode. Furthermore, TEM results show nanostructured SiO₂/NiO/Ni electrocatalysts. The removal efficiency of absorbance and COD of G/SiO₂/NiO/Ni was 100 and 89.94%, respectively, while that of graphite was 99.81 and 78.27%, respectively. The LC-MS analysis showed that the electrochemical removal of RB-5 resulted in the presence of naphthalene, aromatic, and aliphatic compounds with m/z of 41.95, 60.17, 122.60, 143.16, and 152.27. Based on the results, the SiO₂/NiO/Ni nanocomposite electrocatalyst has great potential in the electrochemical oxidation reaction of textile dye waste as it is effective, efficient, effective, and easy to apply.

Nomenclature

C_i the initial COD of RB-5 dye before electrochemical removal (mg L⁻¹)

C_f the COD of RB-5 dye after electrochemical removal (mg L⁻¹)

References

1) M. S. Abdel-Wahed, A. Abdel-Karim, F. H. Margha, and T. A. Gad-Allah, "UV sensitive ZnO and TiO₂-ZnO nanocrystalline transparent glass-ceramic materials for photocatalytic decontamination of surface water and textile industry wastewater," *Environ. Prog. Sustain. Energy.*, **40** (5) 1–11 (2021). doi: 10.1002/ep.13653.

2) D. Jager, D. Kupka, M. Vaclavikova, L. Ivanicova, and G. Gallios, "Degradation of reactive black 5 by electrochemical oxidation," *Chemosphere*, **190**, 405–416 (2017). doi: 10.1016/j.chemosphere.2017.09.126.

3) N. I. I. Zamri, S. L. N. Zulmajdi, E. Kusrini, K. Ayuningtyas, H. M. Yasin, and A. Usman, "Rhodamine B photocatalytic degradation using CuO

particles under uv light irradiation for applications in industrial and medical fields," *Evergreen.*, **7**(2) 280–284 (2020). doi: 10.5109/4055233.

4) A. Azani, D. Halin, M. Al. B. Abdullah, and K. A. Razak, "The effect of GO/TiO_2 thin film during photodegradation of methylene blue dye," *Evergreen.*, **8**(3) 556–564 (2021). doi: 10.5109/4491643.

5) H. Widiyandari, Y. Ayash, M.S. Ja'farawy, A. Subagio, W. B. Widayatno, "Synthesis of WO_3/Pt nanoparticle by microwave-assisted sol-gel method for enhanced photocatalytic property in visible light,"*Evergreen.*, **10**(1) 139-145 (2023). doi:10.5109/6781060

6) R. Muhammad and S. Adityosulindro, "Biosorption of brilliant green dye from synthetic wastewater by modified wild algae biomass," *Evergreen.*, **9**(1) 133–140 (2022). doi: 10.5109/4774228.

7) P. V. Nidheesh, M. Zhou, and M. A. Oturan, "An overview on the removal of synthetic dyes from water by electrochemical advanced oxidation processes," *Chemosphere.*, **197** 210–227 (2018). doi: 10.1016/j.chemosphere.2017.12.195.

8) F. C. Moreira, R. A. R. Boaventura, E. Brillas, and V. J. P. Vilar, "Electrochemical advanced oxidation processes: a review on their application to synthetic and real wastewaters," *Appl. Catal. B Environ.*, **202** 217–261 (2017). doi: 10.1016/j.apcatb.2016.08.037.

9) M. R. Samarghandi, A. Dargahi, A. Shabanloo, H. Z. Nasab, Y. Vaziri, and A. Ansari, "Electrochemical degradation of methylene blue dye using a graphite doped PbO_2 anode: optimization of operational parameters, degradation pathway and improving the biodegradability of textile wastewater," *Arab. J. Chem.*, **13** (8) 6847–6864 (2020). doi: 10.1016/j.arabjc.2020.06.038.

10) M. A. Sandoval, N. Zúñiga-Mallea, L. C. Espinoza, J. Vidal, P. Jara-Ulloa, and R. Salazar, "Decolorization and degradation of a mixture of industrial azo dyes by anodic oxidation using a Ti/Ru0.3Ti0.7O_2 (DSA-Cl_2) electrode," *ChemistrySelect*, **4** (47) 13856–13866 (2019). doi: 10.1002/slct.201903150.

11) R. Ding, X. Li, W. Shi, Q. Xu, L. Wang, H. Jiang, Z.Yang, and E. Liu., "Mesoporous Ni-P nanocatalysts for alkaline urea electrooxidation," *electrochim. Acta.*, **222** 455–462 (2016). doi: 10.1016/j.electacta.2016.10.198.

12) P. P. D. K. Wulan, J. A. Ningtyas, and M. Hasanah, "The effect of nickel coating on stainless steel 316 on growth of carbon nanotube from polypropylene waste," *Evergreen.*, **6**(1) 98–102 (2019). doi: 10.5109/2328411.

13) J. Zhang, D. Zhang, and Y. Liu, "Ni–SiO_2 nanoporous composite as an efficient electrocatalyst for the electrooxidation of hydrogen peroxide," *J. Mater. Sci. Mater. Electron.*, **30** (15) 13895–13909 (2019). doi: 10.1007/s10854-019-01707-0.

14) H. Juliano, F. Gapsari, H. Izzuddin, T. Sudiro, K. Y. Phatama, W. P. Sukmajaya, Zuliantoni, T. M. Putri,

and A. M. Sulaiman, "HA/ZrO_2 coating on CoCr alloy using flame thermal spray," *Evergreen.*, **9**(2) 254–261 (2022). doi: 10.5109/4793632.

15) L. Lei, L. M. Fang, L. F. Zhai, R. Wang, and M. Sun, "Anodic oxidation-assisted O_2 oxidation of phenol catalyzed by Fe_3O_4 at low voltage," *Electrochim. Acta.*, **261** 394–401 (2018). doi: 10.1016/j.electacta.2017.12.155.

16) K. Zhu, H. Qi, X. Sun, and Z. Sun, "Anodic oxidation of diuron using Co_3O_4/Graphite composite electrode at low applied current," *Electrochim. Acta*, **299** 853–862 (2019). doi: 10.1016/j.electacta.2019.01.072.

17) B. Krishnakumar, S. Kumar, J. M. Gil, D. Mani, M. Arivanandhan, and A. J. F. N. Sobral, "Synthesis and characterization of g/Ni–SiO_2 composite for enhanced hydrogen storage applications," *Int. J. Hydrogen Energy*, **44 (**41) 23249–23256 (2019). doi: 10.1016/j.ijhydene.2019.07.073.

18) I. H. Dwirekso, M. Ibadurrohman, and Slamet, "Synthesis of TiO_2-SiO_2-CuO nanocomposite material and its activities for self-cleaning," *Evergreen*, **7**(2) 285–291 (2020). doi: 10.5109/4055234.

19) L. K. Wu and J. M. Hu, "A silica Co-electrodeposition route to nanoporous Co_3O_4 film electrode for oxygen evolution reaction," *Electrochim. Acta*, **116** 158–163 (2014). doi: 10.1016/j.electacta.2013.11.010.

20) F. Basharat, U. A. Rana, M. Shahid, and M. Serwar, "Heat treatment of electrodeposited NiO films for improved catalytic water oxidation," *RSC Adv.*, **5 (**105) 86713–86722 (2015). doi: 10.1039/c5ra17041a.

21) N. M. Wiratini, T. Triyono, W. Trisunaryanti, and A. Kuncaka, "Graphite/NiO/Ni electrode for electro-oxidation of the remazol black 5 dye," *Bull. Chem. React. Eng. Catal.*, **16** (4) 847–856 (2021). doi: 10.9767/bcrec.16.4.11702.847-856.

22) A. N. Popova, "crystallographic analysis of graphite by x-ray diffraction," *Coke Chem.*, **60** (9) 361–365 (2017). doi: 10.3103/S1068364X17090058.

23) Y. R. Dias and O. W. Perez-Lopez, "Carbon dioxide methanation over Ni-Cu/SiO_2 catalysts," *Energy Convers. Manag.*, **203** 112214 (2020). doi: 10.1016/j.enconman.2019.112214.

24) W. Yan, D. Wang, and G. G. Botte,"Electrochemical decomposition of urea with Ni-based catalysts," *Appl. Catal. B Environ.*, **127** 221–226 (2012). doi: 10.1016/j.apcatb.2012.08.022.

25) A. Mukimin, H. Vistanty, and N. Zen, "oxidation of textile wastewater using cylinder Ti/β-PbO_2 electrode in electrocatalytic tube reactor," *Chem. Eng. J.*, **259** 430–437 (2015). doi: 10.1016/j.cej.2014.08.020.

26) Q. Bi, W. Guan, Y. Gao, Y. Cui, S. Ma, and J. Xue, "Study of the mechanisms underlying the effects of composite intermediate layers on the performance of Ti/SnO_2-Sb-La electrodes," *Electrochim. Acta*, **306** 667–679 (2019). doi: 10.1016/j.electacta.2019.03.122.

27) T. Droguett, J. M. Gomez, M. G. Gabaldon, E. Ortega,

S. Mestre, G. Cifuentes, and V. P. Herranz, "Electrochemical degradation of reactive black 5 using two-different reactor configuration," *Sci. Rep.*, **10** (1) 1–11 (2020). doi: 10.1038/s41598-020-61501-5.

28) M. Rivera, M. Pazos, and M. Á. Sanromán, "Development of an electrochemical cell for the removal of reactive black 5," *Desalination*, **274 (**1–3) 39–43 (2011). doi: 10.1016/j.desal.2011.01.074.

29) R. Jinisha, R. Gandhimathi, S. T. Ramesh, P. V. Nidheesh, and S. Velmathi, "Removal of rhodamine B dye from aqueous solution by electro-fenton process using iron-doped mesoporous silica as a heterogeneous catalyst," *Chemosphere*, **200** 446–454 (2018). doi: 10.1016/j.chemosphere.2018.02.117.

30) S. El Aggadi, Z. El Abbassi, and A. El Hourch, "Color removal from dye-containing aqueous solutions by electrooxidation," *Desalin. Water Treat.*, **215** 232–236 (2021). doi: 10.5004/dwt.2021.26766.

31) P. Saxena and J. Ruparelia, "Influence of supporting electrolytes on electrochemical treatability of reactive black 5 using dimensionally stable anode," *J. Inst. Eng. Ser. A*, **100** (2) 299–310 (2019). doi: 10.1007/s40030-019-00360-4.

32) Q. Zhao, F. Wei, L. Zhang, Y. Yang, S. Lv, and Y. Yao, "Electrochemical oxidation treatment of coal tar wastewater with lead dioxide anodes," *Water Sci. Technol.*, **80** (5) 836–845 (2019). doi: 10.2166/wst.2019.323.

33) Y. Tang, D. He, Y. Guo, W. Qu, J. Shang, L. Zhou, R. Pan., and W. Dong., "Electrochemical oxidative degradation of X-6G dye by boron-doped diamond anodes: effect of operating parameters," *Chemosphere*, **258** 127368 (2020). doi: 10.1016/j.chemosphere.2020.127368.

34) Y. Xia, G. Wang, L. Guo, Q. Dai, and X. Ma, "Electrochemical oxidation of acid orange 7 azo dye using a PbO_2 electrode: parameter optimization, reaction mechanism and toxicity evaluation," *Chemosphere*, **241** 125010 (2019). doi: 10.1016/j.chemosphere.2019.125010.

35) B. D. Soni, U. D. Patel, A. Agrawal, and J. P. Ruparelia, "Application of BDD and DSA electrodes for the removal of rb 5 in batch and continuous operation," *J. Water Process Eng.*, **17** 11–21 (2017). doi: 10.1016/j.jwpe.2017.01.009.

36) A. Baddouh, B. El Ibrahimi, M. M. Rguitti, E. Mohamed, S. Hussain, and L. Bazzi, "Electrochemical removal of methylene bleu dye in aqueous solution using Ti/RuO_2–IrO_2 and SnO_2 electrodes," *Sep. Sci. Technol.*, **55 (**10) 1852–1861 (2019). doi: 10.1080/01496395.2019.1608244.

37) Y. Yao, M. Li, Y. Yang, L. Cui, and L. Guo, "Electrochemical degradation of insecticide hexazinone with Bi-doped PbO_2 electrode: influencing factors, intermediates and degradation mechanism," *Chemosphere*, **216** 812–822 (2019). doi: 10.1016/j.chemosphere.2018.10.191.

38) V. M. Vasconcelos, F. L. Ribeiro, F. L. Migliorini, S. A. Suellen, J. R. Steter, M. R. Baldan, and N. G. Neidenei., "Electrochemical removal of reactive black 5 azo dye using non-commercial boron-doped diamond film anodes," *Electrochim. Acta*, **178** 484–493 (2015). doi: 10.1016/j.electacta.2015.07.133.

39) M. R. Samarghandi, D. Nemattollahi, G. Asgari, R. Shokoohi, A. Ansari, and A. Dargahi, "Electrochemical process for 2,4-D herbicide removal from aqueous solutions using stainless steel 316 and graphite anodes: optimization using response surface methodology," *Sep. Sci. Technol.*, **54** (4) 478–493 (2018). doi: 10.1080/01496395.2018.1512618.

40) Y. Yao, Q. Chen, and J. Zhou, "Influence of typical electrolytes on electrooxidation of bio-refractory reactive dye," *Int J Enviro Sci Technol.*, **19** (3) 1799-1810 (2021). doi:10.1007/s13762-021-03184-7.

41) A. J. Méndez-Martínez, M. M. Davila-Jimenez, O. Ornelas-Davila, M. P. Elizalde-Gonzalez, U. Arroyo-Abad, I. Sires, and E. Brillas, "Electrochemical reduction and oxidation pathways for reactive black 5 dye using nickel electrodes in divided and undivided cells," *Electrochim. Acta*, **59 1**40–149 (2012). doi: 10.1016/j.electacta.2011.10.047.